Corrugated, Sheet-Like Architectures in Layered Alkaline-Earth Metal *R,S*-Hydroxyphosphonoacetate Frameworks: Applications for Anticorrosion Protection of Metal Surfaces

Konstantinos D. Demadis,*[,†] Maria Papadaki,[†] Raphael G. Raptis,[‡] and Hong Zhao[‡,§]

Crystal Engineering, Growth and Design Laboratory, Department of Chemistry, University of Crete, Voutes Campus, Heraklion GR-71003, Crete, Greece and Department of Chemistry, University of Puerto Rico at Rio Piedras, San Juan, PR 00931-3346, Puerto Rico

Received April 9, 2008. Revised Manuscript Received May 15, 2008

Reactions of M^{2+} (M = Mg^{2+} (**1**), Ca^{2+} (**2**), Sr^{2+} (**3**), or Ba^{2+} (**4**)) salts with *R,S*-hydroxyphosphonoacetic acid (HPAA) in aqueous solutions of pH 2.0−2.7 at a 1:1 ratio yield hydrated M−HPAA layered or three-dimensional coordination polymers with varying degrees of hydration (metal-coordinated water or lattice water). The crystal structures of **3** (two different phases, **3a** and **3b**, formed at slightly different pH) and **4** have been determined by single-crystal X-ray crystallography. Both enantiomers (*R* and *S*) of HPAA are incorporated in these metal−HPAA materials. Compounds were also characterized by a plethora of other techniques (ATR-IR, SEM, TGA, elemental analyses, powder XRD). Corrosion experiments were carried out at pH 2.0 and 7.3 to study the effect of combinations of externally added Sr^{2+} or Ba^{2+} and HPAA (1:1 ratio) on corrosion rates of carbon steel. It was found that at pH 2.0 Sr/HPAA or Ba/HPAA 1:1 combinations are not able to inhibit corrosion. However, at pH 7.3 quantitative corrosion inhibition is achieved. Anticorrosion films were studied by FT-IR, EDS, and XRF. These amorphous (by XRD) inorganic−organic protective coatings are composed of Sr^{2+} or Ba^{2+} and HPAA in a 1:1 ratio and are identical to Sr−HPAA or Ba−HPAA materials synthesized at pH 7.3 and different from those synthesized at pH 2.0−2.7. Structure elucidation was not possible because they are amorphous.

Introduction

The fields of supramolecular chemistry, crystal engineering, and materials chemistry have seen impressive growth during recent years. Utilization of phosphonic acids ligands has undoubtedly played a key role in widening these areas of research.[1–10] Phosphonate ligands have attracted considerable attention in the context of fundamental research, but have also been extensively used in several other technologically/industrially significant areas, such as water treatment,[11–14] oilfield drilling,[15,16] minerals processing,[17] corrosion control,[18–20] metal complexation and sequestration,[21] dental materials,[22] enzyme inhibition,[23–25] bone targeting,[26–28] cancer treatment,[29] etc. There exists a gamut of metal phosphonate materials whose structures exhibit attractive features that depend on several variables, such as the nature of M^{n+} (metal oxidation state, ionic radius, and coordination number in

* To whom correspondence should be addressed. E-mail: demadis@chemistry.uoc.gr.
† University of Crete.
‡ University of Puerto Rico at Rio Piedras.
§ Present address: Ordered Matter Science Research Center, Southeast University, Nanjing, P.R. China.

(1) (a) Clearfield, A. *Chem. Mater.* **1998**, *10*, 2801–2810. (b) Maeda, K. *Microporous Mesoporous Mater.* **2004**, *73*, 47–55. (c) Demadis, K. D. In *Solid State Chemistry Research Trends*; Buckley, R. W., Ed; Nova Science Publishers: New York, 2007; pp 109−172. (d) Sharma, C. V. K.; Clearfield, A. *J. Am. Chem. Soc.* **2000**, *122*, 4394–4402. (e) Clearfield, A. *Prog. Inorg. Chem.* **1998**, *47*, 371–510.

(2) (a) Vioux, A.; Le Bideau, L.; Hubert Mutin, P.; Leclercq, D. *Top. Curr. Chem.* **2004**, *232*, 145–174. (b) Mahmoudkhani, A. H.; Langer, V. *Phosphorus Sulfur Silicon* **2002**, *177*, 2941–2951. (c) Mahmoudkhani, A. H.; Langer, V. *J. Mol. Struct.* **2002**, *609*, 97–108. (d) Lazar, A. N.; Navaza, A.; Coleman, A. W. *Chem. Commun.* **2004**, 1052–1053. (e) Mahmoudkhani, A. H.; Langer, V. *Cryst. Growth Des.* **2002**, *2*, 21–25.

(3) (a) Du, Z.-Y.; Prosvirin, A. V.; Mao, J.-G. *Inorg. Chem.* **2007**, *46*, 9884–9894. (b) Du, Z.-Y.; Xu, H.-B.; Mao, J.-G. *Inorg. Chem.* **2006**, *45*, 6424–6430. (c) Yang, B.-P.; Mao, J.-G. *Inorg. Chem.* **2005**, *44*, 566–571. (d) Lei, C.; Mao, J.-G.; Sun, Y.-Q.; Zeng, H.-Y.; Clearfield, A. *Inorg. Chem.* **2003**, *42*, 6157–6159.

(4) (a) Cheetham, A. K.; Ferey, G.; Loiseau, T. *Angew. Chem., Int. Ed.* **1999**, *38*, 3268–3272. (b) Forster, P. M.; Cheetham, A. K. *Top. Catal.* **2003**, *24*, 79–86. (c) Merrill, C. A.; Cheetham, A. K. *Inorg. Chem.* **2007**, *46*, 278–284. (d) Jhung, S. H.; Yoon, J. W.; Hwang, J.-S.; Cheetham, A. K.; Chang, J.-S. *Chem. Mater.* **2005**, *17*, 4455–4460. (e) Merrill, C. A.; Cheetham, A. K. *Inorg. Chem.* **2005**, *44*, 5273–5277.

(5) (a) Gomez-Alcantara, M. M.; Cabeza, A.; Martinez-Lara, M.; Aranda, M. A. G.; Suau, R.; Bhuvanesh, N.; Clearfield, A. *Inorg. Chem.* **2004**, *43*, 5283–5293. (b) Cabeza, A.; Ouyang, X.; Sharma, C. V. K.; Aranda, M. A. G.; Bruque, S.; Clearfield, A. *Inorg. Chem.* **2002**, *41*, 2325–2333. (c) Cabeza, A.; Aranda, M. A. G.; Bruque, S. *J. Mater. Chem.* **1999**, *2*, 571–578.

(6) (a) Turner, A.; Jaffres, P.-A.; MacLean, E. J.; Villemin, D.; McKee, V.; Hix, G. B. *J. Chem. Soc., Dalton Trans.* **2003**, 1314–1319. (b) Hix, G. B.; Wragg, D. S.; Wright, P. A.; Morris, R. E. *J. Chem. Soc., Dalton Trans.* **1998**, 3359–3361. (c) Turner, A.; Kariuki, B. M.; Tremayne, M.; MacLean, E. J. *J. Mater. Chem.* **2002**, *11*, 3220–3227. (d) Zakowsky, N.; Hix, G. B.; Morris, R. E. *J. Mater. Chem.* **2000**, *10*, 2375–2380.

(7) (a) Stock, N.; Bein, T. *Angew. Chem., Int. Ed.* **2004**, *43*, 749–752. (b) Bauer, S.; Stock, N. *Angew. Chem., Int. Ed.* **2007**, *46*, 6857–6860. (c) Forster, P. M.; Stock, N.; Cheetham, A. K. *Angew. Chem., Int. Ed.* **2005**, *44*, 7608–7611. (d) Bauer, S.; Bein, T.; Stock, N. *J. Solid State Chem.* **2006**, *179*, 145–155.

(8) (a) Breeze, B. A.; Shanmugam, M.; Tuna, F.; Winpenny, R. E. P. *Chem. Commun.* **2007**, 5185–5187. (b) Langley, S.; Helliwell, M.; Raftery, J.; Tolis, E. I.; Winpenny, R. E. P. *Chem. Commun.* **2004**, 142–143. (c) Baskar, V.; Shanmugam, M.; Sañudo, E. C.; Shanmugam, M.; Collison, D.; McInnes, E. J. L.; Wei, Q.; Winpenny, R. E. P. *Chem. Commun.* **2007**, 37–39. (d) Harrison, A.; Henderson, D. K.; Lovatt, P. A.; Parkin, A.; Tasker, P. A.; Winpenny, R. E. P. *Dalton Trans.* **2003**, 4271–4274.

10.1021/cm801004w CCC: $40.75
Published on Web 07/12/2008

particular), number of phosphonate groups on the ligand backbone, presence of other functional moieties (carboxylate, sulfonate, amine, hydroxyl), and, naturally, process variables (reactant ratio and concentration, temperature, pressure, etc.). Synthesis of metal phosphonates is usually performed in aqueous solutions (or in mixtures of water and a polar organic solvent), so it is not surprising that water is commonly found in their lattice, participating in extensive hydrogen bonding, which is predominant in these architectures resulting in 1-, 2-, and 3-D supramolecular networks.[30] Lastly, it is worth noting that the vast majority of metal phosphonates are coordination polymers, although there are reports of metal phosphonate molecular complexes.

Herein, we describe syntheses of five new alkaline-earth-metal hydroxyphosphonoacetates, M−HPAA (hydroxyphosphonoacetic acid = HPAA, M = Mg, Ca, Sr (two phases), Ba), and structural characterization of three (Sr (two phases) and Ba) of them. These polymeric inorganic−organic hybrids have the general formula $\{M[(HPAA)(H_2O)_x]\cdot(H_2O)_y\}_n$, with x and y determining the amount of metal-coordinated and lattice water, respectively. Crystalline materials containing metal-coordinated $HPAA^{2-}$ are obtained as products from reactions of HPAA and hydrous MCl_2 salts (M = Mg, **1**; Ca, **2**; Sr, **3a**, **3b**; Ba, **4**) in a 1:1 molar ratio under ambient conditions and low pH (2−3). Synthetic efforts were based on simple "electroneutrality" principles, according to which at the synthesis pH the ligand ($HPAA^{2-}$) and metal (M^{2+}) have the same but opposite charges, thus resulting in neutral frameworks. The metal−HPAA compounds (generated in situ) containing Sr^{2+} or Ba^{2+} have been applied as anticorrosion films for the protection of steel metal surfaces.

Phosphonate additives, initially applied as replacements for carcinogenic chromate in metallic corrosion protection, have since then found extensive use.[18–20] There is a consensus in literature reports on a *synergistic* action of dissolved M^{2+} and phosphonates that has been assigned to formation of metal−phosphonate inhibiting films on the metallic surface.[31] Recently, we initiated a systematic effort to study metal−phosphonate films on metal surfaces, focusing on their accurate description at the molecular level.[32–35]

Experimental Section

Materials. All water-soluble metal salts were commercial samples and used without further purification. A racemic mixture of *R,S*-HPAA (50% w/w solution in water) was from Biolab, U.K. Stock solutions of HCl and NaOH (from Riedel de Haen) were used for pH adjustments. In-house, deionized water was used for all syntheses.

Instrumentation. The TGA apparatus was a TGA/SDTA 851-LF 1100-Mettler with the carrier gas being either air or N_2 at a flow of 100 mL/min. Samples were heated from 25 to 800 °C at a heating rate of 7 °C/min in a aluminum pot (volume 30 μL). FT-IR spectra were recorded on a FT-IR Perkin-Elmer FT 1760. ATR-IR spectra were collected on a Thermo-Electron NICOLET 6700 FTIR optical spectrometer. X-ray diffraction data were collected on a SMART 1K CCD diffractometer at 298(2) K with Mo Kα (λ = 0.71073 Å).

(9) (a) Serre, C.; Groves, J. A.; Lightfoot, P.; Slawin, A. M. Z.; Wright, P. A.; Stock, N.; Bein, T.; Haouas, M.; Taulelle, F.; Ferey, G. *Chem. Mater.* **2006**, *18*, 1451–1457. (b) Ferey, G.; Mellot-Draznieks, C.; Serre, C.; Millange, F. *Acc. Chem. Res.* **2005**, *38*, 217–225. (c) Serre, C.; Lorentz, C.; Taulelle, F.; Ferey, G. *Chem. Mater.* **2003**, *15*, 2328–2337. (d) Barthelet, K.; Nogues, M.; Riou, D.; Ferey, G. *Chem. Mater.* **2002**, *14*, 4910–4918.

(10) (a) Alberti, G.; Casciola, M.; Costantino, U.; Vivani, R. *Adv. Mater.* **1996**, *8*, 291–303. (b) Vivani, R.; Alberti, G.; Costantino, F.; Nocchetti, M. *Microporous Mesoporous Mater.* **2008**, *107*, 58–70. (c) Vivani, R.; Costantino, F.; Costantino, U.; Nocchetti, M. *Inorg. Chem.* **2006**, *45*, 2388–2390. (d) Costantino, U.; Nocchetti, M.; Vivani, R. *J. Am. Chem. Soc.* **2002**, *124*, 8428–8434.

(11) Demadis, K. D.; Katarachia, S. D. *Phosphorus Sulfur Silicon* **2004**, *179*, 627–648.

(12) Demadis, K. D.; Lykoudis, P. *Bioinorg. Chem. Appl.* **2005**, *3*, 135–149.

(13) Demadis, K. D. *Phosphorus Sulfur Silicon* **2006**, *181*, 167–176.

(14) Demadis, K. D.; Mavredaki, E. *Environ. Chem. Lett.* **2005**, *3*, 127–131.

(15) (a) Dyer, S. J.; Anderson, C. E.; Graham, G. M. *J. Pet. Sci. Eng.* **2004**, *43*, 259–270. (b) Oddo, J. E.; Tomson, M. B. *Appl. Geochem.* **1990**, *5*, 527–532. (c) Xiao, J. A.; Kan, A. T.; Tomson, M. B. *Langmuir* **2001**, *17*, 4668–4673. (d) Friedfeld, S. J.; He, S.; Tomson, M. B. *Langmuir* **1998**, *14*, 3698–3703.

(16) (a) Tantayakom, V.; Fogler, H. S.; Charoensirithavorn, P.; Chavadej, S. *Cryst. Growth Des.* **2005**, *5*, 329–335. (b) Browning, F. H.; Fogler, H. S. *AIChE J.* **1996**, *42*, 2883–2896. (c) Pairat, R.; Sumeath, C.; Browning, F. H.; Fogler, H. S. *Langmuir* **1997**, *13*, 1791–1798. (d) Tantayakom, V.; Fogler, H. S.; de Moraes, F. F.; Bualuang, M.; Chavadej, S.; Malakul, P. *Langmuir* **2004**, *20*, 2220–2226.

(17) (a) Penard, A.-L.; Rossignol, F.; Nagaraja, H. S.; Pagnoux, C.; Chartier, T. *Eur. J. Ceram. Soc.* **2005**, *25*, 1109–1118. (b) Pearse, M. J. *Miner. Eng.* **2005**, *18*, 139–149.

(18) (a) Sekine, I.; Shimode, T.; Yuasa, M. *Ind. Eng. Chem. Res.* **1992**, *31*, 434–439. (b) Mosayebi, B.; Kazemeini, M.; Badakhshan, A *Br. Corr. J.* **2002**, *37*, 217–224.

(19) (a) Kouznetsov, Yu, I. *Prot. Met.* **2001**, *37*, 434–439. (b) Balaban-Irmenin; Yu, V.; Rubashov, A. M.; Fokina, N. G. *Prot. Met.* **2006**, *42*, 133–136.

(20) (a) Fang, J. L.; Li, Y.; Ye, X. R.; Wang, Z. W.; Liu, Q. *Corrosion* **1993**, *49*, 266–271. (b) Paszternák, A.; Stichleutner, S.; Felhõsi, I.; Keresztes, Z.; Nagy, F.; Kuzmann, E.; Vértes, A; Homonnay, Z.; Petõ, G.; Kálmán, E. *Electrochim. Acta* **2007**, *53*, 337–345.

(21) (a) Biogeochemistry of Chelating Agents. *ACS Symposium Series 910*; Nowack, B., Van Briessen, J. M., Eds; American Chemical Society: Washington, DC, 2005. and references therein. (b) Knepper, T. P. *Trends Anal. Chem.* **2003**, *22*, 708–724.

(22) (a) Miyazaki, K.; Horibe, T.; Antonucci, J. M.; Takagi, S.; Chow, L. C. *Dent. Mater.* **1993**, *9*, 46–50. (b) Atai, M.; Nekoomanesh, M.; Hashemi, S. A.; Amani, S. *Dent. Mater.* **2004**, *20*, 663–668. (c) Nicholson, J. W.; Singh, G. *Biomaterials* **1996**, *17*, 2023–2030. (d) Tschernitschek, H.; Borchers, L.; Geurtsen, W. *J. Prosth. Dent.* **2006**, *96*, 12–12.

(23) Cheng, F.; Oldfield, E. *J. Med. Chem.* **2004**, *47*, 5149–5158.

(24) Temperini, C.; Innocenti, A.; Guerri, A.; Scozzafava, A.; Rusconi, S.; Supuran, C. T. *Bioorg. Med. Chem. Lett.* **2007**, *17*, 2210–2215.

(25) Davini, E; Di Leo, C.; Norelli, F.; Zappelli, P. *J. Biotechnol.* **1993**, *28*, 321–338.

(26) (a) Bottrill, M.; Kwok, L.; Long, N. J. *Chem. Soc. Rev.* **2006**, *35*, 557–571. (b) Finlay, I. G.; Mason, M. D.; Shelley, M. *Lancet Oncol.* **2005**, *6*, 392–400.

(27) Kubicek, V.; Rudovsky, J.; Kotek, J.; Hermann, P.; Vander Elst, L.; Muller, R. N.; Kolar, Z. I.; Wolterbeek, H. T.; Peters, J. A.; Lukeš, I. *J. Am. Chem. Soc.* **2005**, *127*, 16477–16485.

(28) Kung, H.; Ackerhalt, R.; Blau, M. *J. Nucl. Med.* **1978**, *19*, 1027–1031.

(29) (a) Padalecki, S. S.; Guise, T. A. *Breast Cancer Res.* **2002**, *4*, 35–41. (b) Stresing, V.; Daubiné, F.; Benzaid, I.; Mönkkönen, H.; Clézardin, P. *Cancer Lett.* **2007**, *257*, 16–35. (c) Layman, R.; Olson, K.; Van Poznak, C. *Hematol. Oncol. Clinics N. Am.* **2007**, *21*, 341–367.

(30) (a) Clearfield, A. *Curr. Opin. Solid State Mater. Sci.* **2002**, *6*, 495–506. (b) Clearfield, A. *Curr. Opin. Solid State Mater. Sci.* **1996**, *1*, 268–278.

(31) Marin-Cruz, J.; Cabrera-Sierra, R.; Pech-Canul, M. A.; Gonzalez, I. *Electrochim. Acta* **2006**, *51*, 1847–1854.

(32) Demadis, K. D.; Mantzaridis, C.; Raptis, R. G.; Mezei, G. *Inorg. Chem.* **2005**, *44*, 4469–4471.

(33) Demadis, K. D.; Katarachia, S. D.; Koutmos, M. *Inorg. Chem. Commun.* **2005**, *8*, 254–258.

(34) Demadis, K. D.; Lykoudis, P.; Raptis, R. G.; Mezei, G. *Cryst. Growth Des.* **2006**, *6*, 1064–1067.

(35) Demadis, K. D.; Mantzaridis, C.; Lykoudis, P. *Ind. Eng. Chem. Res.* **2006**, *45*, 7795–7800.

Table 1. Bond Distances for Sr−HPAA (3a), Sr−HPAA (3b), and Ba−HPAA (4)[a]

Sr−HPAA (**3a**)		Sr−HPAA (**3b**)		Ba−HPAA (**4**)	
Sr(1)−O(4)	2.5030(17)	Sr(1)−O(2)#1	2.5698(19)	Ba(1)−O(4)#1	2.706(4)
Sr(1)−O(8)	2.570(2)	Sr(1)−O(7)	2.5821(19)	Ba(1)−O(6)	2.724(4)
Sr(1)−O(1)#1	2.5786(17)	Sr(1)−O(4)	2.598(2)	Ba(1)−O(7)	2.782(4)
Sr(1)−O(9)	2.597(2)	Sr(1)−O(8)	2.635(2)	Ba(1)−O(1)	2.791(4)
Sr(1)−O(6)	2.6055(18)	Sr(1)−O(1)#2	2.6472(18)	Ba(1)−O(8)	2.817(5)
Sr(1)−O(5)#2	2.6178(17)	Sr(1)−O(6)	2.6489(19)	Ba(1)−O(3)#2	2.831(4)
Sr(1)−O(7)	2.623(3)	Sr(1)−O(3)#3	2.7271(19)	Ba(1)−O(5)#3	2.855(4)
Sr(1)−O(5)#1	2.6916(18)	Sr(1)−O(5)#4	2.7530(19)	Ba(1)−O(2)#2	2.858(4)
		Sr(1)−O(5)#2	2.761(2)	Ba(1)−O(2)#4	2.915(4)

[a] Symmetry transformations used to generate equivalent atoms. For Sr−HPAA (**3a**): #1 x, $-y + 1/2$, $z - 1/2$; #2 $-x$, $y - 1/2$, $-z + 3/2$; #3 $-x$, $-y$, $-z + 1$; #4 x, $-y + 1/2$, $z + 1/2$; #5 $-x$, $y + 1/2$, $-z + 3/2$. For Sr−HPAA (**3b**) #1 $x + 1/2$, $-y + 1/2$, $z - 1/2$; #2 x - 1/2, $-y + 1/2$, $z - 1/2$; #3 $-x$, $-y + 1$, $-z + 2$; #4 $-x + 1/2$, $y + 1/2$, $-z + 3/2$; #5 $-x$, $-y + 1$, $-z + 1$; #6 $x + 1/2$, $-y + 1/2$, $z + 1/2$; #7 $x - 1/2$, $-y + 1/2$, $z + 1/2$; #8 $-x + 1/2$, $y - 1/2$, $-z + 3/2$. For Ba−HPAA (**4**) #1 $x + 1/2$, $-y + 3/2$, $z - 1/2$; #2 $x - 1/2$, $-y + 3/2$, $z - 1/2$; #3 $-x$, $-y + 1$, $-z + 1$; #4 $-x + 1/2$, $y - 1/2$, $-z + 1/2$; #5 $-x$, $-y + 1$, $-z$; #6 $x + 1/2$, $-y + 3/2$, $z + 1/2$; #7 $-x + 1/2$, $y + 1/2$, $-z + 1/2$; #8 $x - 1/2$, $-y + 3/2$, $z + 1/2$.

Syntheses. Reactions of HPAA with a variety of divalent metal ions (Mg, Ca, Sr, Ba, Zn, Cu, Cd) occur to give M−HPAA materials (see SI). M−HPAA materials with M = Zn, Cu, and Cd will be reported in a future publication. Similar experimental procedures are followed for the synthesis of all alkaline-earth-metal hydroxyphosphonoacetates.

*M−HPAA Syntheses (M = Mg (**1**), Ca (**2**), Sr (**3b**), Ba(**4**)) at pH 2.0.* A quantity of HPAA (0.5 mL of a 50% w/w aqueous solution, 2.195 mmol) is dissolved in deionized water (25 mL), and hydrated metal chloride (2.195 mmol) is added to it stepwise under vigorous stirring. Solution pH is adjusted to 2.0 with 1.0 M NaOH. The clear, slightly yellow solutions are stored at ambient temperature. All reaction solutions precipitate crystalline material after 3 days. If crystallization is left to proceed over 1 week higher yields are obtained (40−60% based on metal, depending on crystallization time and compound). The precipitates are isolated by filtration and air or oven dried.

*Synthesis of Sr[(HPAA)$(H_2O)_3$]·H_2O (**3a**).* The same procedure as given above was followed except that the solution pH was adjusted to 2.7 with 1.0 M NaOH. Large octahedral blocks crystallize after 4 days. Yield: 45% based on Sr. It should be mentioned that if the $BaCl_2 \cdot 2H_2O$ + HPAA reaction is carried out at pH 2.7, Ba[(HPAA)$(H_2O)_2$ (**4**) is obtained as the only product. It appears that the Ba/HPAA system is insensitive to pH.

Synthesis of Fe[(HPAA)(H_2O) at pH 2.0. The same procedure was followed as given above, except that ferrous ammonium sulfate hexahydrate ($Fe^{II}(NH_4)_2(SO_4)_2 \cdot 6H_2O$) is used (2.195 mmol, 0.861 g). Rapid precipitation of an off-white powder occurs that is isolated by filtration and oven dried. Yield: 65% based on Fe. This product is amorphous based on powder XRD measurements.

M−HPAA Syntheses at pH 7.3 (for Sr and Ba). For the pH 7.3 syntheses, a quantity of hydrated strontium or barium chloride (1.76 mmol) is dissolved in deionized water (25 mL) and the pH is adjusted to 7.3 with NaOH (5 and 1 M stock solutions). At the same time HPAA (metal:HPAA at 1:1 molar ratio, 0.4 mL of a 50% w/w aqueous solution) is added to 25 mL of deionized water and the pH is adjusted to 7.3 with NaOH (5 and 1 M stock solutions). Finally, the individual metal chlorides and HPAA solutions are mixed under vigorous stirring (the metal chloride solution is added dropwise to the HPAA solution), and immediate precipitation of white solids is observed. Yields are 50% for Sr−HPAA and 70% for Ba−HPAA (based on metal). The precipitates are isolated by filtration and air or oven dried. Further details on syntheses, elemental analyses, and spectroscopic characterization are included in the SI. These products are amorphous based on powder XRD measurements.

Synthesis of Fe[(HPAA)(H_2O)] at pH 7.3. The same procedure was followed as given above except that ferrous ammonium sulfate hexahydrate ($Fe^{II}(NH_4)_2(SO_4)_2 \cdot 6H_2O$) (4.39 mmol, 1.722 g) and 1.0 mL (4.39 mmol) of a 50% w/w HPAA aqueous solution are used. Rapid precipitation of an off-white powder occurs that is isolated by filtration and oven dried. Yield: 72% based on Fe. This product is amorphous based on powder XRD measurements.

Crystallography. A table that contains collection and refinement data has been included in the SI. Table 1 contains bond distances and Table 2 bond angles for all three structures. Copies of crystallographic data (cif files) for the structures may be obtained free of charge from the CCDC: Sr−HPAA (**3a**) ref no. 607004, Sr−HPAA (**3b**) ref no. 615683, and Ba−HPAA (**4**) ref no. 614291.

Corrosion Inhibition Protocol. A modified protocol is used based on NACE Standard TM0169-95 (Item No. 21200), National Association of Corrosion Engineers, Houston, TX.[36] Corrosion specimens (carbon steel, grade C1010) are prepared according to the well-established protocol above. Each specimen (pretreated carbon steel C1010) is immersed in a control solution (no inhibitor) or test solution (17.56 mM M^{2+} and 17.56 mM HPAA at pH = 2.0 or 1.76 mM M^{2+} and 1.76 mM HPAA at pH = 7.3), and corrosion progress is monitored by visual inspection for 6 days. Lower concentrations for the pH = 7.3 experiments are used to avoid bulk precipitation of the metal−HPAA materials. Then, the specimens are removed from solution, surface samples are taken for spectroscopic studies, and corrosion products are cleaned by the standard NACE method above to determine corrosion rates from mass loss.

Results and Discussion

Syntheses. A generalized reaction can be written as follows (proton content on the HPAA ligand is also shown in bold[37])

$$M^{2+} + R,S-\mathbf{H}O_2CCH(O\mathbf{H})PO_3\mathbf{H}_2 + \text{excess } H_2O \xrightarrow{pH = 2-2.7} \{M[R,S-(O_2CCH(O\mathbf{H})PO_3\mathbf{H})(H_2O)_x]\cdot(H_2O)_y\}_n + 2\mathbf{H}^+$$

where M = Mg $x = 2$, $y = 0$ (**1**); M = Ca $x = 2$, $y = 0$ (**2**); M = Sr $x = 3$, $y = 1$ (**3a**); M = Sr $x = 2$, $y = 0$ (**3b**); M = Ba $x = 2$, $y = 0$ (**4**). At pH ≈ 2.7 HPAA possesses a "2−" overall charge ($HPAA^{2-}$) with each carboxylic and phosphonic acid group being singly deprotonated.[37] In principle, its association with M^{2+} cations leads to neutral, polymeric materials. However, anionic metal−HPAA frame-

(36) NACE Standard TM0169-95 (Item No. 21200), National Association of Corrosion Engineers, Houston, TX; www.nace.org.
(37) pK_a's of H_3PAA: 1.2, 4.8, 7.93. Stunzi, H.; Perrin, D. D. *J. Inorg. Biochem.* **1979**, *10*, 309–316.

Table 2. Bond Angles for Sr−HPAA (3a), Sr−HPAA (3b), and Ba−HPAA (4)

Sr−HPAA (3a)		Sr−HPAA (3b)		Ba−HPAA (4)	
O(4)−Sr(1)−O(8)	81.76(7)	O(2)#1−Sr(1)−O(7)	137.25(6)	O(4)#1−Ba(1)−O(6)	136.97(10)
O(4)−Sr(1)−O(1)#1	70.13(5)	O(2)#1−Sr(1)−O(4)	140.46(6)	O(4)#1−Ba(1)−O(7)	137.79(10)
O(8)−Sr(1)−O(1)#1	134.35(7)	O(7)−Sr(1)−O(4)	76.19(6)	O(6)−Ba(1)−O(7)	78.63(11)
O(4)−Sr(1)−O(9)	98.96(7)	O(2)#1−Sr(1)−O(8)	69.35(7)	O(4)#1−Ba(1)−O(1)	70.92(11)
O(8)−Sr(1)−O(9)	76.33(9)	O(7)−Sr(1)−O(8)	130.80(6)	O(6)−Ba(1)−O(1)	68.25(9)
O(1)#1−Sr(1)−O(9)	73.56(7)	O(4)−Sr(1)−O(8)	107.24(8)	O(7)−Ba(1)−O(1)	146.08(10)
O(4)−Sr(1)−O(6)	74.09(6)	O(2)#1−Sr(1)−O(1)#2	87.50(6)	O(4)#1−Ba(1)−O(8)	69.11(13)
O(8)−Sr(1)−O(6)	78.46(8)	O(7)−Sr(1)−O(1)#2	87.88(7)	O(6)−Ba(1)−O(8)	105.52(15)
O(1)#1−Sr(1)−O(6)	124.09(7)	O(4)−Sr(1)−O(1)#2	70.73(6)	O(7)−Ba(1)−O(8)	132.34(11)
O(9)−Sr(1)−O(6)	154.57(8)	O(8)−Sr(1)−O(1)#2	140.60(6)	O(1)−Ba(1)−O(8)	66.66(11)
O(4)−Sr(1)−O(5)#2	155.09(5)	O(2)#1−Sr(1)−O(6)	72.21(6)	O(4)#1−Ba(1)−O(3)#2	86.08(12)
O(8)−Sr(1)−O(5)#2	77.55(6)	O(7)−Sr(1)−O(6)	145.57(6)	O(6)−Ba(1)−O(3)#2	70.32(11)
O(1)#1−Sr(1)−O(5)#2	134.75(5)	O(4)−Sr(1)−O(6)	70.27(5)	O(7)−Ba(1)−O(3)#2	88.42(13)
O(9)−Sr(1)−O(5)#2	89.55(8)	O(8)−Sr(1)−O(6)	68.69(6)	O(1)−Ba(1)−O(3)#2	74.04(12)
O(6)−Sr(1)−O(5)#2	88.18(6)	O(1)#2−Sr(1)−O(6)	74.14(6)	O(8)−Ba(1)−O(3)#2	138.45(11)
O(4)−Sr(1)−O(7)	106.14(11)	O(2)#1−Sr(1)−O(3)#3	131.66(6)	O(4)#1−Ba(1)−O(5)#3	133.06(9)
O(8)−Sr(1)−O(7)	139.67(9)	O(7)−Sr(1)−O(3)#3	69.82(6)	O(6)−Ba(1)−O(5)#3	74.04(10)
O(1)#1−Sr(1)−O(7)	83.83(10)	O(4)−Sr(1)−O(3)#3	71.54(6)	O(7)−Ba(1)−O(5)#3	67.54(12)
O(9)−Sr(1)−O(7)	137.92(8)	O(8)−Sr(1)−O(3)#3	65.56(7)	O(1)−Ba(1)−O(5)#3	108.36(13)
O(6)−Sr(1)−O(7)	66.61(8)	O(1)#2−Sr(1)−O(3)#3	139.71(6)	O(8)−Ba(1)−O(5)#3	68.32(11)
O(5)#2−Sr(1)−O(7)	81.69(12)	O(6)−Sr(1)−O(3)#3	105.59(6)	O(3)#2−Ba(1)−O(5)#3	140.24(10)
O(4)−Sr(1)−O(5)#1	130.56(5)	O(2)#1−Sr(1)−O(5)#4	80.92(6)	O(4)#1−Ba(1)−O(2)#2	72.01(11)
O(8)−Sr(1)−O(5)#1	135.75(8)	O(7)−Sr(1)−O(5)#4	69.77(6)	O(6)−Ba(1)−O(2)#2	116.32(11)
O(1)#1−Sr(1)−O(5)#1	60.47(5)	O(4)−Sr(1)−O(5)#4	138.35(6)	O(7)−Ba(1)−O(2)#2	70.75(11)
O(9)−Sr(1)−O(5)#1	70.03(7)	O(8)−Sr(1)−O(5)#4	79.30(7)	O(1)−Ba(1)−O(2)#2	117.44(10)
O(6)−Sr(1)−O(5)#1	133.11(6)	O(1)#2−Sr(1)−O(5)#4	129.46(6)	O(8)−Ba(1)−O(2)#2	136.36(14)
O(5)#2−Sr(1)−O(5)#1	74.35(6)	O(6)−Sr(1)−O(5)#4	143.66(6)	O(3)#2−Ba(1)−O(2)#2	54.83(9)
O(7)−Sr(1)−O(5)#1	67.97(8)	O(3)#3−Sr(1)−O(5)#4	74.65(6)	O(5)#3−Ba(1)−O(2)#2	133.69(9)
		O(2)#1−Sr(1)−O(5)#2	71.26(6)	O(4)#1−Ba(1)−O(2)#4	82.95(12)
		O(7)−Sr(1)−O(5)#2	70.33(6)	O(6)−Ba(1)−O(2)#4	139.71(9)
		O(4)−Sr(1)−O(5)#2	118.40(6)	O(7)−Ba(1)−O(2)#4	69.01(12)
		O(8)−Sr(1)−O(5)#2	133.85(7)	O(1)−Ba(1)−O(2)#4	143.81(9)
		O(1)#2−Sr(1)−O(5)#2	58.12(5)	O(8)−Ba(1)−O(2)#4	81.02(12)
		O(6)−Sr(1)−O(5)#2	119.75(5)	O(3)#2−Ba(1)−O(2)#4	129.84(10)
		O(3)#3−Sr(1)−O(5)#2	134.45(5)	O(5)#3−Ba(1)−O(2)#4	71.83(12)
		O(5)#4−Sr(1)−O(5)#2	71.60(6)	O(2)#2−Ba(1)−O(2)#4	75.27(10)

works with fully deprotonated tri-anionic $HPAA^{3-}$ have been reported with divalent metal ions, albeit these incorporate an organoammonium cation (vide infra) for charge balance. Water content (either metal coordinated or in the lattice) is variable. It cannot be predicted a priori for each synthesis. Syntheses at pH 7.3 (they were only limited to Sr, Ba, and Fe) rapidly produce amorphous precipitates; thus, crystallization of products suitable for single-crystal X-ray analyses was not possible. These products are distinctly different from those synthesized at pH 2.0 (based on FT-IR, elemental analyses, and powder XRD). A slight change in solution pH (from 2.0 to 2.7) leads to formation of another phase of Sr−HPAA (**3b**). It should be noted that this change in pH has no effect on the Ba−HPAA system, yielding **4** in both cases.

Crystallography. The identity of **3a**, **3b**, and **4** has been confirmed by single-crystal X-ray crystallography. Crystallographic data are presented in Table 4.1 (see SI, collection and refinement) and Tables 1 (bond distances) and 2 (bond angles). The structural descriptions for materials **3a**, **3b**, and **4** are presented below.

*Sr[(HPAA)(H_2O)$_3$]·H_2O (**3a**).* This is a 2-D, layered polymer consisting of "Sr(HPAA)(H_2O)$_3$" units that are connected through a Sr−O(carboxylate) linker. The Sr atoms are 8-coordinated. Sr−O bond distances range from 2.5030(17) to 2.6916(18) Å. Consequently, each $HPAA^{2-}$ ligand is coordinated to three symmetry-related Sr^{2+} centers (Figure 1, top). On the basis of the virtually equal C−O bond lengths (C(2)−O(5) 1.258(3) Å and C(2)−O(6) 1.260(3) Å) the negative charge is delocalized over the entire O−C−O moiety. The Sr−$O_{carboxylate}$ bond distances are 2.6055(18) (monodentate), 2.6178(17) (bridging), and 2.6916(18) Å

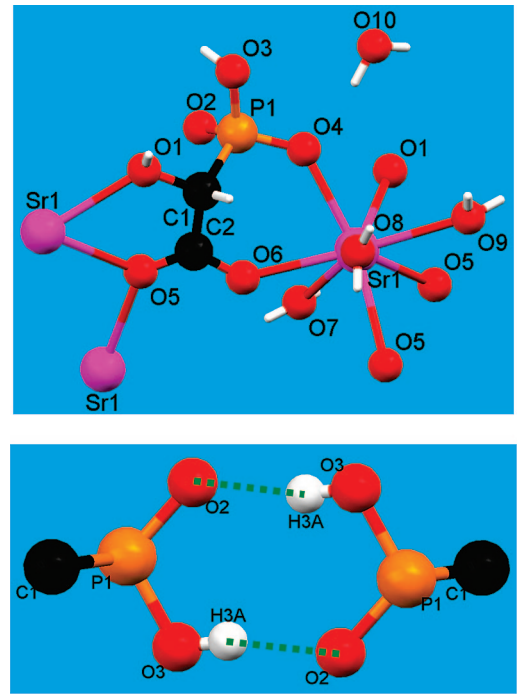

Figure 1. Coordination environment of Sr in **3a** showing the multiple bridging of HPAA (top). Hydrogen-bonded phosphonate dimer between two adjacent layers (bottomo). Color code: Sr, magenta; P, orange; C, black; O, red; H, white.

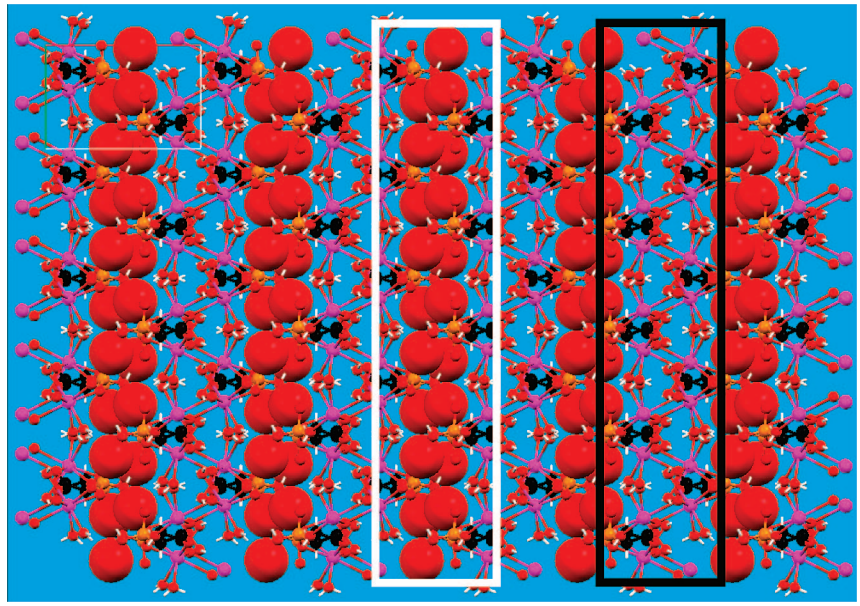

Figure 2. Layered structure of Sr−HPAA (**3a**) seen along the *c* axis with exaggerated lattice water molecules (red spheres in the white box) separating the Sr−HPAA layers (in the black box). Color code: Sr, magenta; P, orange; C, gray; O, red.

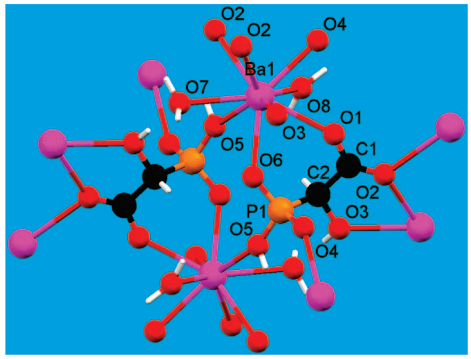

Figure 3. Coordination environment of Ba^{2+} centers in **4** showing the multiple bridging of HPAA. Color code: M (Sr, Ba), magenta; P, orange; C, black; O, red; H, white.

(bridging). The monodeprotonated $-PO_3H^-$ group is coordinated to only one Sr with a Sr−O(4) bond distance of 2.5030(17) Å. The P−O bond lengths (P−O(4) 1.5000(17) Å, P−O(2) 1.516(2) Å, and P−O_H(3) 1.5680(17) Å) point to delocalization of the negative charge over the O(4)−P−O(2) moiety. The hydroxyl group remains protonated with its oxygen atom found at a 2.5786(17) Å from Sr. The coordination environment of Sr could best be described as a bicapped octahedron. There is one H_2O of crystallization per asymmetric unit. O−Sr−O angles range from 70.13(5)° to 98.96(7)°. Each HPAA acts as a double chelate bridge between two Sr ions (a carboxyl and the hydroxyl oxygens chelate one Sr, while the other carboxyl and a phosphono oxygen chelate another Sr). This type of HPAA bridging induces sufficient "strain" to create a zigzag chain with alternating "Sr" and "HPAA" units with a Sr−Sr−Sr dihedral angle of 136.27°. These zigzag chains are connected through Sr−O(carboxyl) linkages found on every other Sr, thus creating a corrugated layer that runs parallel to the bc plane. One could envision this architecture as a "double inorganic layer", the bridging mode of the carboxylate oxygen O(5) being responsible for it. The closest Sr···Sr *intralayer* contact is 4.231 Å, whereas the closest Sr···Sr *interlayer* contact is 7.150 Å. Neighboring layers are connected through extensive hydrogen-bonding interactions that involve the water molecule of crystallization (Figure 2). Specifically, O(10) forms four hydrogen bonds, O(10)···O(4) 2.743 Å (with the Sr-coordinated O−P moiety), O(10)···O(1) 2.712 Å (with the Sr-bound hydroxyl moiety), O(10)···O(9) 2.754 Å (with a Sr-coordinated water), and O(10)···O(2) 2.919 Å (with the "free" O−P moiety). Furthermore, the neighboring "double layers" interact additionally via hydrogen bonds that include two noncoordinating −(O)P−O−H moieties from two adjacent layers (Figure 1, bottom). These −(O)P−O−H groups form two identical hydrogen bonds O(2)···O(3) 2.599 Å, creating a local P−O−H···O−P dimer, reminiscent of the classical "carboxylic acid dimer".[38]

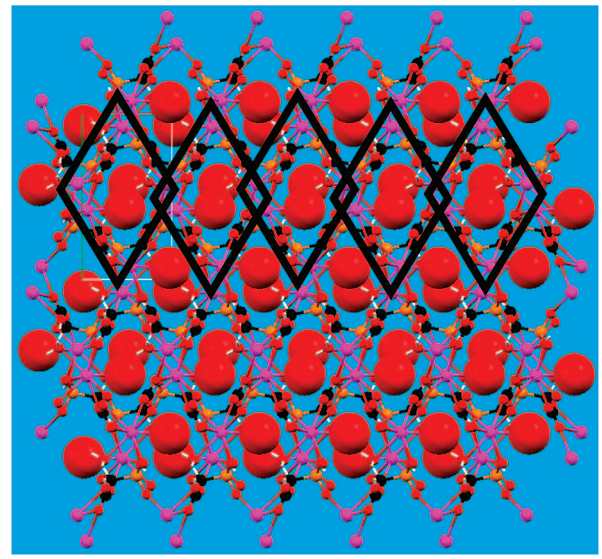

Figure 4. 3-D structure of Ba−HPAA (**4**) showing packing along the *c* axis and the Ba-coordinated waters (exaggerated O8) filling the "pores" (shown schematically as rhombs). Color code: M (Sr, Ba), magenta; P, orange; C, gray; O, red.

*M(HPAA)(H_2O)$_2$ (M = Sr (**3b**), Ba (**4**).* Materials **3b** and **4** are isostructural. In the 3-D structure of **4**, each HPAA

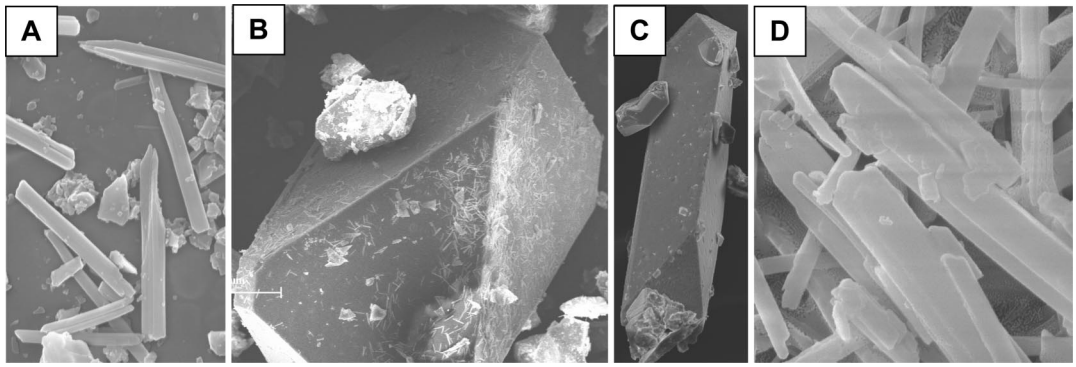

Figure 5. SEM images of Ca−HPAA (**2**, A), Sr−HPAA (**3a**, B), Sr−HPAA (**3b**, C), and Ba−HPAA (**4**, D). Width of images (in μm) = 60 (A), 10 (B), 20 (C), and 5 (D).

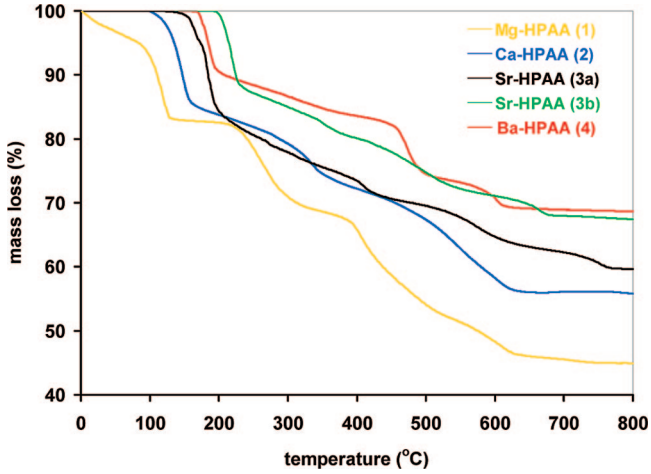

Figure 6. Thermogravimetric curves for compounds **1**, **2**, **3a**, **3b**, and **4**.

links to five symmetry-equivalent, 9-coordinated Ba^{2+} centers through its phosphonate group (bridging three Ba ions), the carboxylate group (bridging two Ba), and the protonated hydroxyl moiety (coordinating terminally one Ba center), Figure 3. There are no H_2O's of crystallization but only two Ba-coordinated waters (O(7) and O(8)) in the structure. The $Ba-OH_2$ bond distances are 2.782(4) and 2.817(5) Å. $Ba-O_{carboxylate}$bond distances are 2.971(4) (monodentate), 2.858(4) (bridging), and 2.914(4) Å (bridging). The C−O bond lengths (C(1)−O(1) 1.273(4) and C(1)−O(2) 1.235(5) Å) suggest delocalization of the negative charge over both O carboxyl atoms. The monodeprotonated $-PO_3H^-$ group is coordinated to three Ba atoms in a bridging μ_3 mode with bond distances of Ba−O(4) 2.706(4) Å, $Ba-O_H(5)$ 2.855(4) Å, and Ba−O(6) 2.724(4) Å. O(5) bears the H atom. This is supported by the P−O bond lengths: P−O(4) 1.513(3) Å, P−O(5) 1.572(3) Å, and P−O(6) 1.484(3) Å. The near equivalency of the two P−O bond lengths (P−O(4) and P−O(6)) point to delocalization of the negative charge over the O(4)−P−O(6) moiety. The hydroxyl group remains protonated with its oxygen atom found at a 2.831(4) Å from Ba. The coordination environment of Ba could be best described as a distorted bicapped trigonal antiprism. The hydroxyl (O(3)) and one carboxyl oxygen (O(2)) create a five-membered ring with Ba, whereas one phosphono oxygen (O(6)) and the other carboxyl oxygen (O(1)) create a six-membered ring with a neighboring Ba. The multiple coordination ability of the $-PO_3H^-$ moiety in the structure of **4**(**3b**) can be contrasted to the monodentate coordination mode of the $-PO_3H^-$ group in **3a**. In the latter, the absence of the bridging capability of the $-PO_3H^-$ group creates a layered structure, whereas in the former the bridging μ_3 mode of the $-PO_3H^-$ group is responsible for generation of a three-dimensional motif.

In all structures both *R* and *S* HPAA isomers are incorporated in the layers. In **3a**, each "double" layer is *R*-*S*-*R*-*S*-. In **3b(4)**, the *R* and *S* isomers are interwoven into a complicated 3-D arrangement (Figure 4).

The 3-D structure of **4** is also supported by several hydrogen bonds that form between the −OH, −P−O−H, and Ba-coordinated waters. Specifically, the hydroxyl O(3) creates a hydrogen bond with two Ba-bound waters, O(7) and O(8) (at 2.675 and 2.894 Å). The protonated −P−O−H group is hydrogen bonded to Ba-bound carboxyl O(1) (at 2.522 Å). Ba-coordinated water, O(8), is hydrogen bonded simultaneously to another Ba-bound water, O(7) (2.758 Å), and the hydroxyl, O(3) (2.894 Å). The second Ba-coordinated water, O(7), forms three hydrogen bonds simultaneously with another Ba-bound water, O(8) (2.758 Å), with the hydroxyl group, O(3) (2.675 Å), and with a Ba-coordinated phosphoryl, O(4) (2.654 Å).

A number of metal−HPAA structures have been reported for various transition metals but are distinctly different than those reported herein, mainly due to incorporation of amine templating agents into the final solid and the presence of other metal-coordinated ligands or a second metal ion used in syntheses.[39–48] Neutral metal−HPAA compounds that contain only HPAA and water as ligands (absence of other ligands) include the recently published isostructural series of $M(HPAA)(H_2O)_2$ (M = Mn, Fe, Co, Zn).[41] These materials appear to have the same elemental composition (i.e., one metal center, one doubly deprotonated HPAA ligand, and two metal-coordinated water molecules) as **3b** and **4**. However, important factors such the octahedral coordination geometry of the metal centers, monodentate coordination of the carboxylate group, and absence of a bond between the protonated −P−O−H group and the metal center lead to a different structure (layered vs three dimensional) from **3b** and **4**. In addition, a $Ni(HPAA)(H_2O)_2$ compound was reported to have one-dimensional structure.[45]

(38) Demadis, K. D.; Raptis, R. G.; Baran, P. *Bioinorg. Chem. Appl.* **2005**, *3*, 119–134.

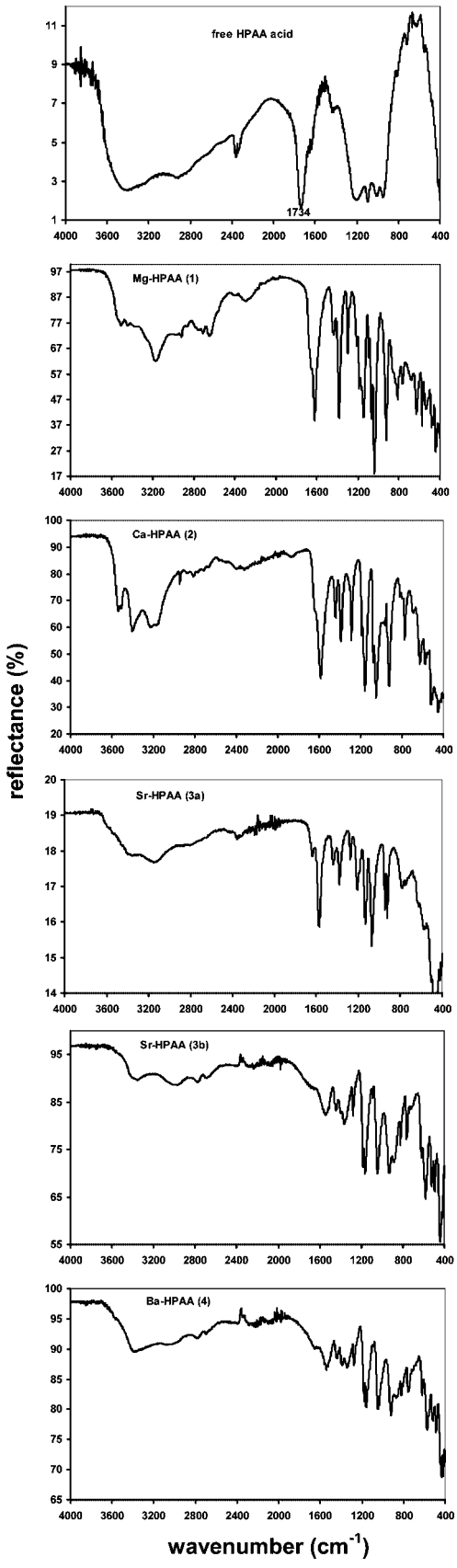

Figure 7. ATR-IR spectra of compounds **1**−**4**.

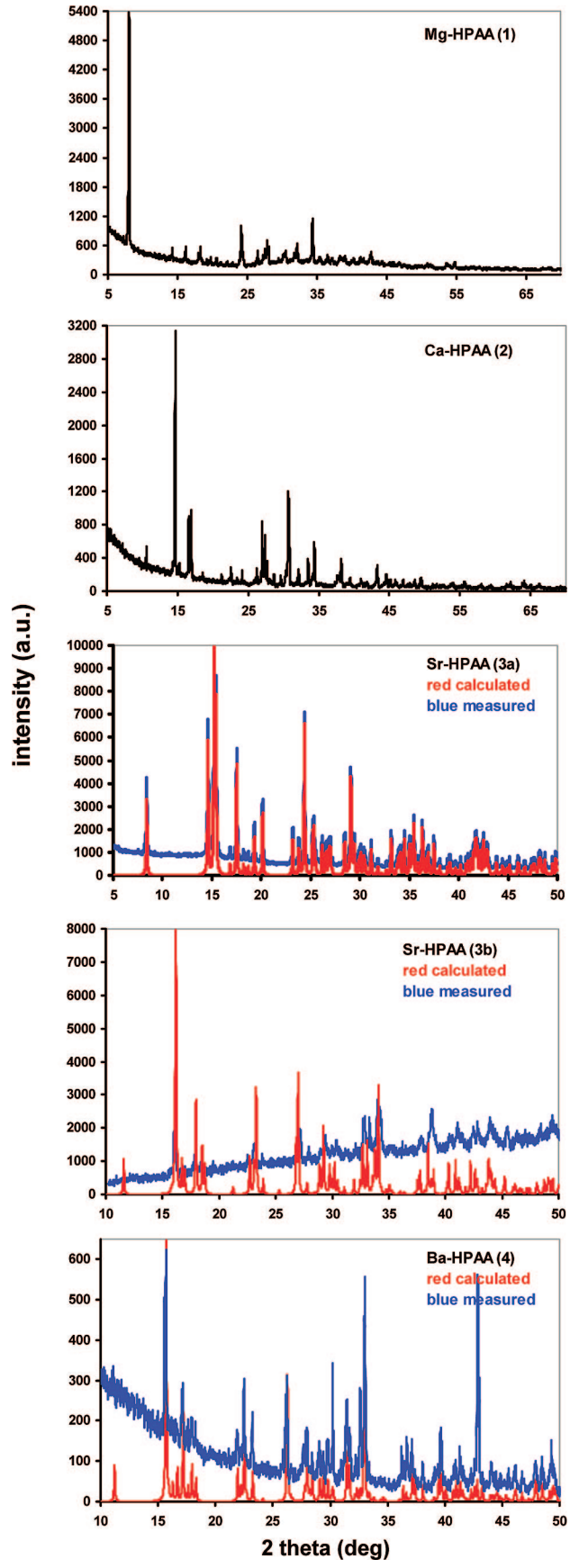

Figure 8. XRD patterns of compounds **1**−**4**. For crystallographically characterized compounds calculated patterns are presented as well.

Miscellaneous Characterization Methods (SEM, TGA, Powder XRD, and FT-IR). All materials reported herein were also characterized by other techniques, such as SEM, TGA, powder XRD, and FT-IR. SEM images of four representative materials are shown in Figure 5. These reveal that the compounds studied show well-defined crystal edges

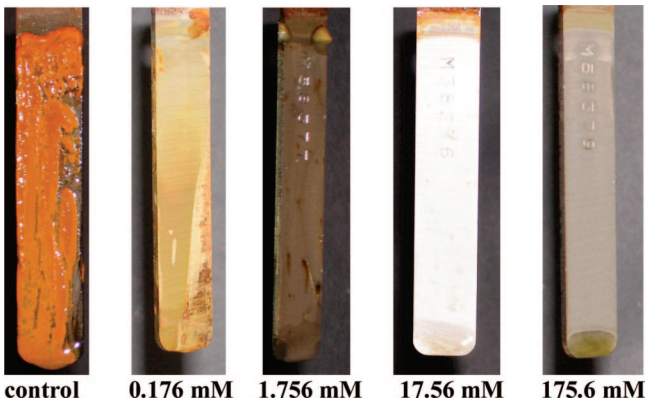

Figure 9. Concentration-dependent effect of free HPAA on carbon steel. Although metal specimens corresponding to [HPAA] 17.56 and 175.6 mM appear free from corrosion products, corrosion rates are very high, leading to severe metal dissolution (see text and Table 3).

and surfaces. Thermogravimetric analysis was employed to study removal of water molecules (metal-bound and lattice) and compound thermal decomposition. The results are shown in Figure 6. All materials were studied under air and under nitrogen gas without variation in the results obtained. Water loss in Mg−HPAA (**1**) is initiated at room temperature and continues up to ∼135 °C. Mass loss of ∼16.10%, corresponding to removal of both water molecules (15.59% theoretical), produces an amorphous compound. Ca−HPAA (**2**) starts losing water at ∼100 °C, and this loss continues until ∼165 °C, where two water molecules are removed (calculated loss 15.65%, measured loss 15.30%). Further temperature increase results in HPAA ligand decomposition. Full decomposition occurs until 625 °C. We studied water loss from Ca−HPAA (**2**) thermodiffractometrically (results not shown here, see SI). After 90 °C the material starts losing crystallinity, and at 120 °C it is completely amorphous.

Mass loss for Sr−HPAA (**3b**) is initiated at ∼195 °C, showing a well-defined loss until 245 °C. This loss clearly corresponds to removal of two water molecules (calculated loss 12.97%, measured loss 12.53%). As temperature increases gradual mass loss occurs with no discernible steps. Mass loss ceases at ∼680 °C. Mass loss for Ba−HPAA (**4**) starts at ∼170 °C, showing an abrupt drop until ∼214 °C. This loss fits well with removal of two water molecules (calculated loss 10.99%, measured loss 10.79%). After this temperature, ligand decomposition occurs that is complete at ∼620 °C. Again, for this compound there are no temperature ranges where mass remains unchanged. Thus, isolation and characterization of possible dehydrated "intermediates" is not an option for compounds **2**, **3b**, and **4**. Following water loss, decomposition of HPAA occurs for all compounds by release of CO_2. The measured mass losses that are due to HPAA degradation correspond well to the calculated ones. These are 21.9% (21.0 calculated) for **1**, 20.3% (19.0% calculated) for **2**, 14.8% (14.1% calculated) for **3a**, 15.5% (15.8% calculated) for **3b**, and 13.4% (13.7% calculated) for **4**. Final, metal-containing products after heat treatment at 800 °C have not been characterized. If formation of $M(HPO_4)$ is assumed, the following decomposition can be envisioned in air after removal of lattice waters

$$M[(O_2CCH(OH)(PO_3H)](s) + 3/2O_2(g) \rightarrow M(HPO_4)(s) + 2CO_2(g) + H_2O(g)$$

Vibrational spectroscopy was employed as well to further characterize these compounds. Attenuated total reflectance (ATR) spectra are shown in Figure 7. This technique[49] as well as routine FT-IR[50] were successfully employed for the study of metal−phosphonocarboxylate inorganic−organic hybrids. Mid-IR spectra (400−4000 cm^{-1} region) of metal−HPAA products display a multitude of bands in the region 1100−1270 cm^{-1} assigned to the P═O stretch and intense bands in the regions 1500−1650 (due to $\nu(C{=}O)_{asym}$) and 1340−1450 cm^{-1} (due to $\nu(C{=}O)_{sym}$). Free HPAA shows the $\nu(C{=}O)_{asym}$ stretch as an intense sharp band at 1734 cm^{-1} and the $\nu(P{=}O)$ and $\nu(P{-}O)$ stretches as intense, overlapping bands in the 900−1250 cm^{-1} region. Spectra of isostructural compounds **3b** and **4** are virtually identical with only minor changes, as expected. Both $\nu(C{=}O)_{asym}$ and $\nu(C{=}O)_{sym}$ vibrations appear in similar positions for **3a** and **3b**(**4**) (1573, 1547, and 1549 cm^{-1}, respectively, for $\nu(C{=}O)_{asym}$ and 1379, 1369, and 1349 cm^{-1}, respectively, for $\nu(C{=}O)_{sym}$). This observation is consistent with the structural results. In all three structures the $-COO^-$ moiety displays the same mode of coordination to the metal centers (see structural description, vide supra). However, severe broadening of the $\nu(C{=}O)_{asym}$ band in the spectra of **3b** and **4** is notable (see Figure 7) compared to the sharp $\nu(C{=}O)_{asym}$ band in the spectrum of **3a**. A possible explanation for this could be the presence of a strong hydrogen bond between the carboxyl O(1) and the protonated O(5) −P−OH group (2.522 Å) in the structure of **3b** and **4**. This is in contrast to the behavior of the carboxyl O's (5 and 6), which do not participate in any hydrogen bonds. The POO^- stretching vibration appears at 1211 (**3a**), 1185 (**3b**), and 1180 cm^{-1} (**4**). It has been suggested[50] that such values indicate that the −P═O double bond is delocalized, in accordance with our structural findings for the three structures. A doublet in the region 920−970 cm^{-1} is assigned to the −P−OH

(39) Fu, R.; Zhang, H.; Wang, L.; Hu, S.; Li, Y.; Huang, X.; Wu, X. *Eur. J. Inorg. Chem.* **2005**, 3211–3213.
(40) Zhang, Y.-Y.; Zeng, M.-H.; Qi, Y.; Sang, S.-Y.; Liu, Z.-M. *Inorg. Chem. Commun.* **2007**, *10*, 33–36.
(41) Fu, R.; Xiang, S.; Zhang, H.; Zhang, J.; Wu, X. *Cryst. Growth Des.* **2005**, *5*, 1795–1799.
(42) Sun, Z.-G.; Chen, H.; Liu, Z.-M.; Cui, L.-Y.; Zhu, Y.-Y.; Zhao, Y.; Zhang, J.; You, W.-S.; Zhu, Z.-M. *Inorg. Chem. Commun.* **2007**, *10*, 283–286.
(43) Li, J.; Meng, L.; Sun, Z.-G.; Cui, L.-Y.; Zhang, J.; Zhang, Y.-Y.; Dong, D.-P.; Chen, H.; You, W.-S.; Zhu, Z.-M. *Inorg. Chem. Commun.* **2007**, *10*, 535–537.
(44) Sun, Z.-G.; Cui, L.-Y.; Liu, Z.-M.; Meng, L.; Chen, H.; Dong, D.-P.; Zhang, L.-C.; Zhu, Z.-M.; You, W.-S. *Inorg. Chem. Commun.* **2006**, *9*, 999–1001.
(45) Li, J.; Dong, D.-P.; Huang, C.-Y.; Sun, Z.-G.; Zhu, Y.-Y. *Acta Crystallogr., Sect. E* **2007**, *E63*, m2348–m2349.
(46) Sun, Z.-G.; Cui, L.; Chen, H.; Meng, L.; Dong, D.; Tian, C.; Zhu, Z.; You, W. *J. Coord. Chem.* **2007**, *60*, 1247–1254.
(47) Zhao, Q.-H.; Dua, L.; Fang, R.-B. *Acta Crystallogr., Sect. E* **2006**, *E62*, m219–m221.
(48) Sun, Z.-G.; Dong, D.-P.; Li, J.; Cui, L.-Y.; Zhu, Y.-Y.; Zhang, J.; Zhao, Y.; You, W.-S.; Zhu, Z.-M. *J. Coord. Chem.* **2007**, *60*, 2541–2547.
(49) Chaplais, G.; Le Bideau, J.; Leclercq, D.; Vioux, A. *Chem. Mater.* **2003**, *15*, 1950–1956.
(50) Zima, V.; Svoboda, J.; Benes, L.; Melanova, K.; Trchova, M.; Dybal, J. *J. Solid State Chem.* **2007**, *180*, 929–939.

Table 3. Corrosion Rates Obtained in the Absence (Control) and Presence of Combinations of M^{2+} (Sr or Ba) and HPAA

free HPAA or metal−HPAA material	concentration (mM)	corrosion rates (CR, × 10^{-3} mm/yr)			
		pH = 2.0		pH = 7.3	
control		299	0% inhibition	142	0% inhibition
HPAA	0.176			41	27.3% inhibition
HPAA	1.76	155	48.1% inhibition	73	48.6% inhibition
HPAA	17.56	492	metal dissolution	192	metal dissolution
HPAA	175.6			466	metal dissolution
Sr+HPAA[b]	*b*	465	metal dissolution[a]	0.48	99.7% inhibition[a]
Ba+HPAA[b]	*b*	397	metal dissolution[a]	0.46	99.7% inhibition[a]

[a] % Inhibition is defined as $[(CR_{control} - CR_{inhibitor})/CR_{control}] \times 100$. [b] Concentrations used: $[Sr^{2+}] = [Ba^{2+}] = [HPAA] = 17.56$ mM (metal:HPAA in a 1:1 molar ratio) for pH = 2.0 and $[Sr^{2+}] = [Ba^{2+}] = [HPAA] = 1.76$ mM (metal:HPAA in a 1:1 molar ratio) for pH = 7.3. Lower concentrations for the pH = 7.3 experiments are used to avoid bulk precipitation of the metal−HPAA materials.

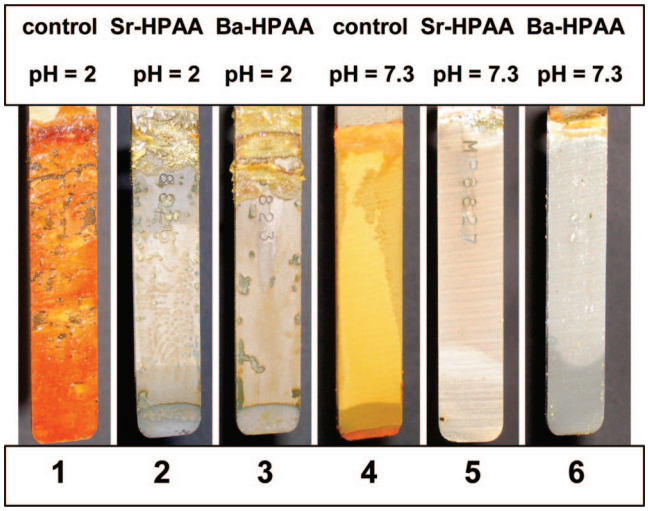

Figure 10. Anticorrosion effect of metal−HPAA films on carbon steel. Corrosion inhibition by metal−HPAA synergistic combinations is evident (specimens **2**, **3**, **5**, and **6**) compared to the "control" (specimens **1** and **4**). Although specimens **2** and **3** (pH = 2.0) are free of iron oxides, corrosion rates are higher than the "control" (see text).

antisymmetric and symmetric stretching vibrations. The strong band in the region 1045−1072 cm^{-1} is tentatively assigned to an antisymmetric vibration mode of the $-CPO_3$ group. Bands in the spectra for all metal−HPAA compounds are also observed in the 400−550 cm^{-1} region. These are assigned to the $-PO_3$ symmetric and $-PO_3$ antisymmetric bending modes.

All metal−HPAA compounds were also characterized by powder XRD, and the patterns are presented in Figure 8. Patterns for **3b** and **4** are almost identical, as expected, since these compounds are isostructural. All other patterns are different, suggesting different structures. Unfortunately, compounds **1** and **2** have not as of yet been structurally characterized.

Corrosion Inhibition Studies. Corrosion experiments were performed to verify previous literature reports on the synergy of metal ions and phosphonate additives and study the protective film acting as a corrosion barrier. First, we attempted to establish the concentration-dependent effect of free HPAA on carbon steel at two different pH's, 2.0 and 7.3 (see Figure 9 and Table 3). It was found that there is an optimum concentration for inhibition performance (1.756 mM, 0.073 mm/y for pH 7.3). Decreasing [HPAA] to 0.176 mM results in a decrease in performance (0.041 mm/y at pH 7.3). Importantly, an increase in [HPAA] to 17.56 and 175.6 mM has a detrimental effect on the anticorrosion performance and causes Fe metal dissolution (192 and 466 mm/y, respectively, at pH 7.3).

Initial experiments with metal/HPAA mixtures were focused on exposure of carbon steel specimens to synergistic combinations of M^{2+} (Sr or Ba) and HPAA in oxygenated aqueous solutions in a 1:1 ratio (under identical conditions used to prepare crystalline M−HPAA at pH 2.0). Although the visual effect was at first encouraging (Figure 10, compare the "control" specimen **1** with specimens **2** and **3**), quantification of the corrosion rates demonstrated that they were actually much higher than the "control" (Table 3).

Explanations for this lack of anticorrosion performance at low pH regions could be that the HPAA added first reacts preferentially with the Fe−oxide layer (formed almost instantaneously upon exposure of the carbon steel surface to oxygenated water) before it interacts with soluble Sr^{2+} or Ba^{2+}. Another possibility is that Sr−HPAA or Ba−HPAA compounds that may form in solution never reach the steel surface because they undergo bulk precipitation. We discounted this scenario based on the following arguments. Indeed, we observed white precipitates formed in the bulk in our corrosion experiments (pH 2.0) whose FT-IR, however, is distinctly different from those of authentically prepared Sr−HPAA or Ba−HPAA (see SI). These FT-IR spectra are the same as that of a Fe−HPAA material prepared at pH 2.0 using a Fe:HPAA ratio of 1:1, whose composition is consistent with the formula $Fe(HPAA)\cdot H_2O$. A reasonable assumption is that HPAA at the surface acts as an Fe−oxide dissolving agent. We observed a similar behavior in similar experiments with M^{2+} (M = Ca, Zn) and 2-phosphonobutane-1,2,4-tricarboxylic acid (PBTC).[34] On the other hand, results published on the action of combinations of metal ions (Ca^{2+} or Zn^{2+}) with HEDP (HEDP = hydroxyethylidene-1,1-diphosphonic acid) on carbon steel revealed that Ca^{2+} was displaced by Fe^{2+} in a "low-stability" Ca−HEDP complex.[51] This did not occur for the Zn−HEDP case, resulting in a much more effective corrosion protection in the "Zn + HEDP system". The Zn/phenylphosphonate system (note the presence of only one phosphonate group in phenylphosphonate vs two in HEDP) showed an analogous Zn^{2+} for Fe^{3+} exchange.[52] A similar process of Sr^{2+} or Ba^{2+} displacement by Fe^{3+} could be envisioned in our case. This can explain the formation of Fe−HPAA precipitates at pH 2.0 but no Sr−HPAA or Ba−HPAA. Due to the ineffective-

(51) Awad, H. S.; Turgoose, S. *Corrosion* **2004**, *60*, 1168–1179.
(52) Rajendran, S.; Apparao, B. V.; Palaniswamy, N. *Anti-Corros. Method. Mater.* **1998**, *45*, 158–161.

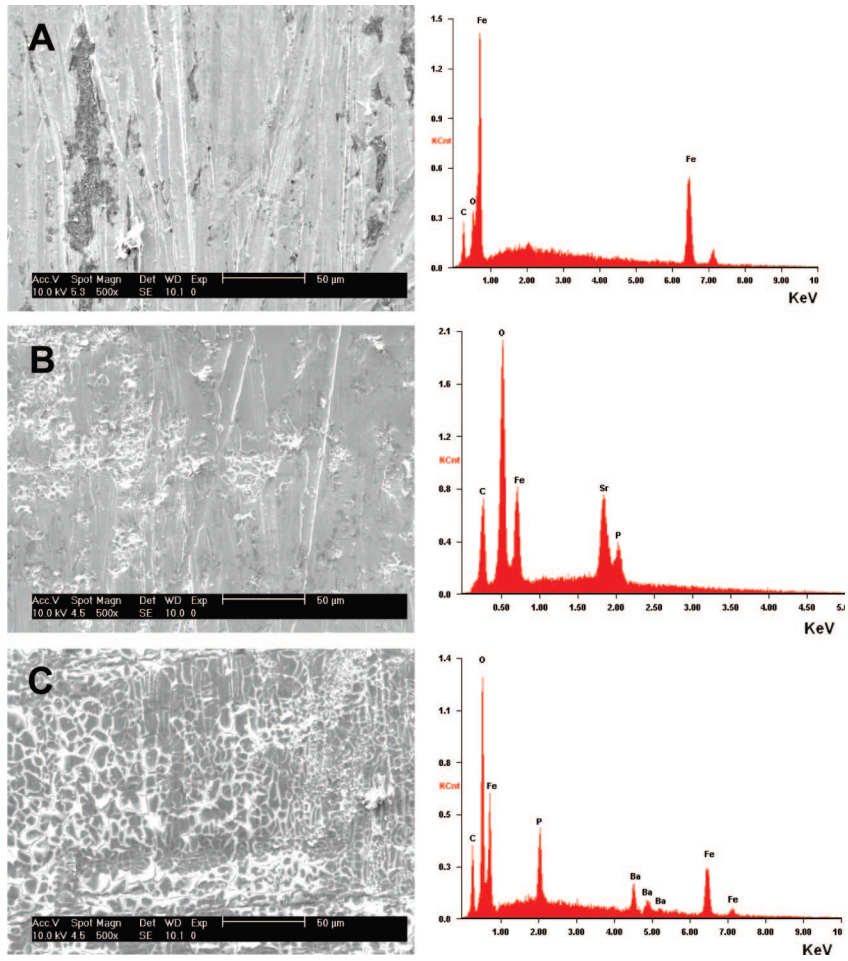

Figure 11. Micromorphology of corroded and metal−HPAA-protected steel surfaces as revealed by SEM: control (A), Sr−HPAA (B), and Ba−HPAA (C) at pH 7.3. Occasional film cracking is due to drying. Identification of film components (Fe, C, O, Sr, Ba, and P) was possible by EDS.

ness of the metal−HPAA materials to act as corrosion inhibitors at pH 2.0, no further experiments were pursued at that pH.

Hence, corrosion experiments were set up at higher pH 7.3. In general, corrosion rates are lower as pH increases.[53] This was confirmed in our "control" experiments (reduction of the corrosion rate by one-half, see Table 3 and specimens **1** and **4** in Figure 10). At higher pH (7.3) and in the presence of Sr^{2+} or Ba^{2+} and HPAA combinations corrosion rates are dramatically suppressed and corrosion inhibition reaches almost 100% (Table 3). Although differentiation between the "control" and "metal−HPAA"-protected specimens is profound within the first hours, the corrosion experiments were left to proceed over a 6-day period. Anticorrosion inhibitory activity was based on mass-loss measurements.[36] Anticorrosion performance was also demonstrated by visual inspection of specimens **5** and **6** that appear totally free of corrosion products. To further characterize the protective film the corrosion specimens and film material were subjected to SEM, FT-IR, XRF, and EDS studies (Figure 11).

SEM images (Figure 11, left) reveal a fairly uniform inhibiting film. This coating was found (by EDS, Figure 11, right) to contain M^{2+} (Sr or Ba from externally added salts) and P (from added HPAA) in an approximate 1:1 molar ratio. Fe was also present, apparently originating from the carbon steel specimen. Further, a complementary study of the inhibiting film was pursued by FT-IR spectroscopy. Figure 12 shows comparative FT-IR spectra of the filming material (from a corrosion experiment with Sr^{2+} and HPAA at pH 7.3) and a Sr−HPAA material that was synthesized at pH 7.3. A similar FT-IR spectrum was obtained for the Ba^{2+} + HPAA system (see SI).

It is obvious that there is an excellent agreement between the two spectra. Comparison of the FT-IR spectra in Figure 12 and those (for **3a**, **3b**, and **4**) in Figure 7 indicates that the molecular structure of the filming material is *not* the same as the structurally characterized materials **3a**, **3b**, and **4**. Although the film displays a $\nu(C{=}O)_{asym}$ vibration at 1582 cm^{-1} that is at a similar position with that of **3a**, **3b**, and **4** (1573, 1547, and 1549 cm^{-1}, respectively), the $\nu(C{=}O)_{sym}$ vibration at 1408 cm^{-1} is distinctly different from that of **3a**, **3b**, and **4** (1379, 1369, and 1349 cm^{-1}, respectively). This difference may originate from a change in the coordination mode of the carboxylate moiety in the filming material.

Notably, the region associated with bands due to the phosphonate group has undergone dramatic changes. The doublet at 925 and 948 cm^{-1} in the spectrum of **3a**, assigned to the −P−OH antisymmetric and symmetric stretching vibrations, has completely disappeared in the spectrum of the film and given rise to a new band at 976 cm^{-1}. This

(53) Sastri, V. S. *Corrosion Inhibitors, Principles and Applications*; John Wiley & Sons: Chichester, 1998; p 737.

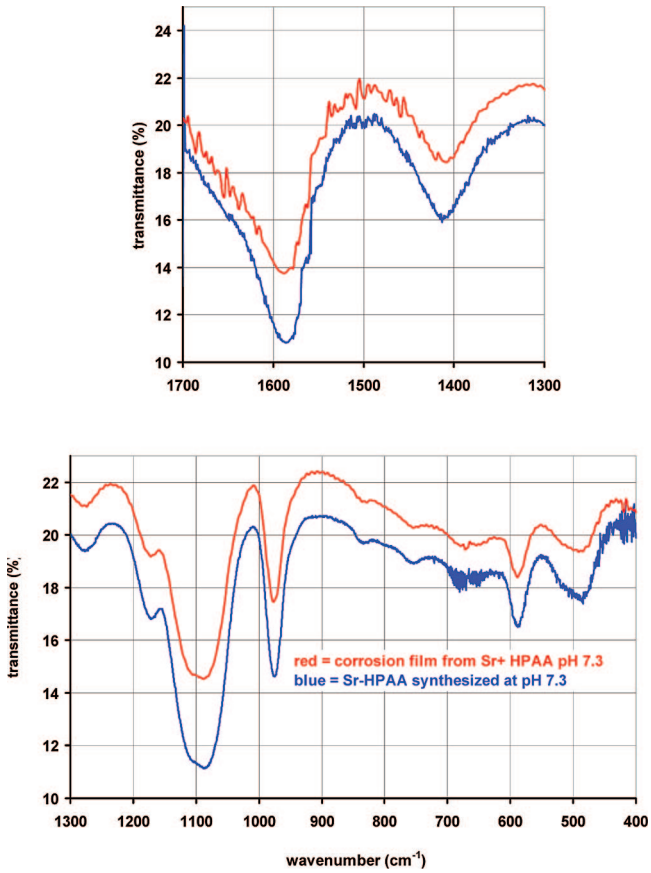

Figure 12. FT-IR of the anticorrosion protective film formed by combination of Sr^{2+} and HPAA at pH 7.3 and, for comparison, of Sr−HPAA synthesized at pH 7.3. (Top) ν(C═O) asymmetric and symmetric stretching vibrations. (Bottom) vibrations associated with the phosphonate group.

implies that coordination of the −P−OH group is different in the film from that in **3a**. Similar observations can be made after comparison of the FT-IR spectrum of the Sr−HPAA film and that of **3b**. There are various shifts in several other peaks as well. Therefore, most likely, the molecular structure of the Sr−HPAA film (and by inference of the Ba−HPAA film) is different from that of **3b** (or **4**) as well. Several attempts to synthesize Sr−HPAA and Ba−HPAA materials at pH ≈ 7 have given powders but not crystalline products. These compounds are amorphous by powder XRD. Therefore, at present, the true molecular structures of these films cannot be accurately determined based on available data. We will not make an attempt to propose a possible structure, as this would be highly hypothetical. Nevertheless, attempts to crystallize Sr−HPAA and Ba−HPAA materials at pH ≈ 7 are under way.

The anticorrosion coatings composed of Sr−HPAA or Ba−HPAA function as corrosion inhibitors by reducing the cathodic current (see SI). This results in lower corrosion rates. The films prevent oxygen diffusion toward the steel surface. This phenomenon is well known for phosphonate additives.[54] To our knowledge, there is no systematic study published that focuses on a "structure/function" relationship of corrosion inhibitors. It is widely accepted that the presence of phosphonate groups is necessary for good anticorrosion performance because these are responsible for metal−phosphonate film formation, via coordination.[55] However, the role of other groups present on the phosphonate backbone (e.g., hydroxyl, carboxyl, amine, etc.) is poorly understood. Several literature reports, however, report high inhibition efficiencies for phosphonates that contain other groups besides a single phosphonate moiety, such as multiple phosphonate groups, hydroxyl, and carboxyl.[56] Obviously, further research is needed to elucidate the true role of these additional groups in anticorrosion efficiency.

Conclusions

The principal highlights/conclusions of this research are given below: (a) a conveniently synthesized under mild conditions and structurally characterized series of divalent metal−HPAA (Mg^{2+} (**1**), Ca^{2+} (**2**), Sr^{2+} (**3**), or Ba^{2+} (**4**), HPAA = *R,S*-hydroxyphosphonoacetic acid) organic−inorganic hybrid polymeric materials is described. (b) Their structures show some variability with slight changes in pH, creating 2-D layered structures (**3a**) or 3-D architectures (**3b** and isostructural **4**). (c) When metal−HPAA compounds (Sr^{2+} or Ba^{2+}) are generated in situ at pH 2.0 in an aqueous solution in contact with a carbon steel specimen, they are unable to inhibit metallic corrosion and, in fact, corrosion rates are dramatically increased compared to the "control". This was assigned to preferential formation of Fe(III)−HPAA compounds that abstract the Fe^{3+} cations from the steel specimen, thus facilitating metal loss and mitigating metal dissolution. (d) When metal−HPAA compounds (Sr^{2+} or Ba^{2+}) are generated in situ at circumneutral pH they act as effective corrosion inhibitors (with inhibition efficiency ≈ 100%) by creating anticorrosion protective films on the carbon steel surface composed of Sr−HPAA or Ba−HPAA hybrids. These are not the same compounds as those synthesized at pH 2.0 (and structurally characterized).

Although the field of metal phosphonate chemistry has progressed impressively over the past decade, it is far from

(54) (a) Gunasekaran, G.; Palanisamy, N.; Appa Rao, B. V.; Muralidharan, V. S. *Electrochim. Acta* **1997**, *42*, 1427–1434. (b) Kalman, E.; Lukovits, I.; Palinkas, G. *ACH-Models in Chemistry* **1995**, *132*, 527–537. (c) Bofardi, B. P. In *Reviews on Corrosion Inhibitor Science and Technology*; Raman, A., Labine, P., Eds.; NACE International: Houston, TX, 1993; p II-6. (d) Kuznetsov, Y. I.; Kazanskaya, G. Y.; Tsirulnikova, N. V. *Prot. Met.* **2003**, *39*, 120–123. (e) Benabdellah, M.; Dafali, A.; Hammouti, B.; Aouniti, A.; Rhomari, M.; Raada, A.; Sehaji, O.; Robin, J. J. *Chem. Eng. Commun.* **2007**, *194*, 1328–1341.

(55) Gunasekaran, G.; Natarajan, R.; Muralidharan, V. S.; Palaniswamy, N.; Appa Rao, B. V. *Anti-Corros. Method. Mater.* **1997**, *44*, 248–259.

(56) (a) Amar, H.; Benzakour, J.; Derja, A.; Villemin, D.; Moreau, B.; Braisaz, T. *Appl. Surf. Sci.* **2006**, *252*, 6162–6172. (b) Felhõsi, I.; Kálmán, E. *Corros. Sci.* **2005**, *47*, 695–708. (c) Pech-Canul, M. A.; Bartolo-Pérez, P. *Surf. Coat. Technol.* **2004**, *184*, 133–140. (d) Amar, H.; Benzakour, J.; Derja, A.; Villemin, D.; Moreau, B. *J. Electroanal. Chem.* **2003**, *558*, 131–139. (e) Felhõsi, I.; Telegdi, J.; Pálinkás, G.; Kálmán, E. *Electrochim. Acta* **2002**, *47*, 2335–2340. (f) Nakayama, N. *Corros. Sci.* **2000**, *42*, 1897–1920. (g) Shaban, A.; Kálmán, E.; Biczó, I. *Corros. Sci.* **1993**, *35*, 1463–1470. (h) Paszternák, A.; Stichleutner, S.; Felhõsi, I.; Keresztes, Z.; Nagy, F.; Kuzmann, E.; Vértes, A.; Homonnay, Z.; Petõ, G.; Kálmán, E. *Electrochim. Acta* **2007**, *53*, 337–345. (i) Salasi, M.; Shahrabi, T.; Roayaei, E.; Aliofkhazraei, M. *Mater. Chem. Phys.* **2007**, *104*, 183–190. (j) Ramesh, S; Rajeswari, S.; Maruthamuthu, S *Appl. Surf. Sci.* **2004**, *229*, 214–225. (k) Ramesh, S; Rajeswari, S.; Maruthamuthu, S. *Mater. Lett.* **2003**, *57*, 4547–4554. (l) Gunasekaran, G.; Natarajan, R.; Palaniswamy, N. *Corros. Sci.* **2001**, *43*, 1615–1626. (m) To, X. H.; Pebere, N.; Pelaprat, N.; Boutevin, B.; Hervaud, Y. *Corros. Sci.* **1997**, *39*, 1925–1934.

maturity. There are still a plethora of opportunities in basic research[57] and other application areas, such as biotechnology,[58] hydrogen storage,[59] scale inhibition,[60] bone resorption,[61] catalytic oxidations,[62] ionic conductors,[63] pro-drugs,[64] anticalcification agents,[65] intercalation,[66] ion adsorption,[67] and several others. Further development of this growing field of materials chemistry is dependent on (poly)phosphonate ligand availability through organic synthesis.[68]

Acknowledgment. We thank the Department of Chemistry, University of Crete, and the GSRT (contract # 2006-207c) for financial support and Biolab Water Additives for a sample of HPAA. Technical assistance from V. Ramos, A. Cabeza, and A. Popa is also gratefully acknowledged.

Supporting Information Available: Various views of the structures, far and mid FT-IR spectra, and XRD powder patterns for all compounds, crystallographic details (bond distances and angles) (PDF), and cif files of **3** (**a** and **b**) and **4** (PDF). This material is available free of charge via the Internet at http://pubs.acs.org.

CM801004W

(57) (a) Clearfield, A. *J. Alloys Compd.* **2006**, *418*, 128–138. (b) Bauer, S.; Bein, T.; Stock, N. *Inorg. Chem.* **2005**, *44*, 5882–5889. (c) Stock, N.; Bein, T. *J. Mater. Chem.* **2005**, *15*, 1384–1391. (d) Gomez-Alcantara, M. M.; Aranda, M. A. G.; Olivera-Pastor, P.; Beran, P.; Garcia-Munoz, J. L.; Cabeza, A. *Dalton Trans.* **2006**, 577–585.

(58) Bujoli, B.; Lane, S. M.; Nonglaton, G.; Pipelier, M.; Leger, J.; Talham, D. R.; Tellier, C. *Chem. Eur. J.* **2005**, *11*, 1980–1988.

(59) (a) Brunet, E.; Alhendawi, H. M. H.; Cerro, C.; de la Mata, M. J.; Juanes, O.; Rodriguez-Ubis, J. C. *Angew. Chem., Int. Ed.* **2006**, *45*, 6918–6920. (b) Brunet, E.; Cerro, C.; Juanes, O.; Rodriìguez-Ubis, J. C.; Clearfield, A. *J. Mater. Sci.* **2008**, *43*, 1155–1158.

(60) Kofina, A. N.; Demadis, K. D.; Koutsoukos, P. G. *Cryst. Growth Des.* **2007**, *7*, 2705–2712.

(61) Zeevaart, J. R.; Jarvis, N. V.; Louw, W. K. A.; Jackson, G. E. *J. Inorg. Biochem.* **2001**, *83*, 57–65.

(62) Vasylyev, M.; Neumann, R. *Chem. Mater.* **2006**, *18*, 2781–2783.

(63) Alberti, G.; Casciola, M.; D'Alessandro, E.; Pica, M. *J. Mater. Chem.* **2004**, *14*, 1910–1914.

(64) Marma, M. S.; Kashemirov, B. A.; McKenna, C. E. *Bioorg. Med. Chem. Lett.* **2004**, *14*, 1787–1790.

(65) (a) Demadis, K. D.; Sallis, J. D.; Raptis, R. G.; Baran, P. *J. Am. Chem. Soc.* **2001**, *123*, 10129–10130. (b) Sallis, J. D.; Demadis, K. D.; Cheung, H. S. *Curr. Rheum. Rev.* **2006**, *2*, 95–99. (c) Sun, Y.; Reuben, P.; Wenger, L.; Sallis, J. D.; Demadis, K. D.; Cheung, H. S. *Front. Biosci.* **2005**, *10*, 803–813.

(66) Lazarin, A. M.; Airoldi, C. *Thermochim. Acta* **2005**, *437*, 114–120.

(67) Wu, J.; Hou, H.; Han, H.; Fan, Y. *Inorg. Chem.* **2007**, *46*, 7960–7970.

(68) (a) Jones, K. M. E.; Mahmoudkhani, A. H.; Chandler, B. D.; Shimizu, G. K. H. *CrystEngComm* **2006**, *8*, 303–305. (b) Turhanen, P.; Demadis, K. D.; Peräniemi, S.; Vepsäläinen, J. *J. Org. Chem.* **2007**, *72*, 1468–1471. (c) Morin, C. J.; Carli, M.; Mofaddel, N.; Al Rifaï, R.; Jaffrès, P. A.; Villemin, D.; Desbène, P. L. *Chromatografia* **2005**, *62*, 139–143. (d) Princz, E.; Szilágyi, I.; Mogyorósi, K.; Labádi, I. *J. Therm. Anal. Calorim.* **2002**, *69*, 427–439.